



Employing Machine Learning to Analyze NSAIDs Drug Similarity via Sombor Invariants

Abaid ur Rehman Virk¹, Iftikhar Ahmed^{2,✉}, Murat Cancan³

¹ *Department of Mathematics, University of Management and Technology, Lahore, Pakistan*

² *University of Agriculture, Faisalabad, Burewala Campus, Pakistan*

³ *Faculty of Education, Yuzuncu Yil University, Van, Turkey*

ABSTRACT

This study introduces a novel approach to investigating Sombor indices and applying machine learning methods to assess the similarity of non-steroidal anti-inflammatory drugs (NSAIDs). The research aims to predict the structural similarities of nine commonly prescribed NSAIDs using a machine learning technique, specifically a linear regression model. Initially, Sombor indices are calculated for nine different NSAID drugs, providing numerical representations of their molecular structures. These indices are then used as features in a linear regression model trained to predict the similarity values of drug combinations. The model's prediction performance is evaluated by comparing the predicted similarity values with the actual similarity values. Python programming is employed to verify accuracy and conduct error analysis.

Keywords: Sombor index, Machine Learning Algorithm, Linear regression model, Nonsteroidal anti-inflammatory drugs (NSAIDs)

2020 Mathematics Subject Classification: 05C15, 05C38, 05C76.

1. Introduction

All of us have occasionally used painkillers in our lives. Painkillers can be used to ease a variety of acute and chronic pains. Sudden acute discomfort subsides once the underlying cause is resolved. However, chronic pain can persist for weeks or even months at a time, leading to a prolonged reliance

✉ Corresponding author.

E-mail addresses: iftikhar.ahmed@uaf.edu.pk (Iftikhar Ahmed).

Received 30 September 2024; accepted 14 December 2024; published 31 December 2024.

DOI: [10.61091/um121-08](https://doi.org/10.61091/um121-08)

© 2024 The Author(s). Published by Combinatorial Press. This is an open access article under the CC BY license (<https://creativecommons.org/licenses/by/4.0/>).

on opioids [9]. While the majority of people think that opioids are safe, long-term or excessive use may be harmful to one's health. The human body has hundreds of nerves that communicate with one another to send messages. Although nerves are found all over the body, their terminals, also known as nerve endings, are restricted to the skin, gastrointestinal tract, and connective tissues. Analgesics, the term used in medicine to describe painkillers, can work in one of two ways: Prostaglandins should not be released since they block the brain's ability to perceive pain [20]. To prevent pain signals from reaching the brain, sever the connection between the two nerves. These processes allow for the temporary reduction or alleviation of pain with the use of medication. The two main categories into which painkillers fall are non-prescription (over-the-counter) and prescription. The most popular types of painkillers range depending on their capacity to reduce pain:

- Nonsteroidal anti-inflammatory drugs (NSAIDs).
- Non-opioid relievers.
- Opioid relievers.
- Mixed painkillers.

This study focus on the analysis of NSAID drugs. Despite their widespread use, NSAIDs can not be taken by everyone and can occasionally have undesirable side effects [5]. If you feel unease in one or more muscles or joints in a particular body part, it may be valuable to use NSAID gels and creams that you nourish into your skin because compared to tablets or capsules, they typically have less negative effects . Chemical graph theory is a field of mathematical chemistry focused on the study of chemical graphs, which represent and characterize chemical structures. [1, 21, 22] A best tool of chemical graph theory is a topological index, that play a crucial rule in binding the mathematical concept with chemistry [4, 3, 16]. While conducting this study, a diversity of pharmaceuticals are engross, and then, by use invariants depending upon the degree of nodes, For each of these medications, a variety of topological indicators are developed to ascertain their unique characteristics and corresponding chemical processes. Chemists and pharmacists might use the resources offered by graph theory for further study, such as Quantitative Structure-Activity/Property/Toxicity Relationship (QSAR/QSPR/QSTR). QSAR modeling is employed to determine the biological activity of the structures [18]. Husin et al. [11] gives the topological analysis of certain networks.

Lately, studies have concentrated on topological indexes for pharmaceutical, and QSAR has been utilized to discuss and present a number of findings. Topological indices are important considerations in the physio-chemical analysis of chemical compound structures [15, 19]. On a graph, a chemical compound's constituents are often illustrated as vertices, while the bonds that link them are portrayed as edges. As on the same steps, The NSAID drugs that are the subject of this investigation are regarded as chemicals, and the topological indices are defined. Additionally, we show that there is a high correlation between the obtained features and those of NSAIDs using regression analysis. In chemistry, the concepts of valence and in graph theory idea of degree are somewhat related. These days, QSPR plays an crucial part in the process of drug design. This is because they are a more affordable substitute for the conventionally employed medium throughput in vitro and low throughput in vivo testing. Environmental toxicity and drug development are two areas where QSAR models are becoming more widely accepted as a valid scientific approach for anticipate and characterization of biological poisonings of unexamined substances, as well as for predicting drug toxicity, resistance, and physicochemical qualities. In the field of chemistry, drugs are portrayed as networks of molecules, where each edge denotes a link between two atoms and each vertex represents an atom [2, 25, 6].

Most of the time, the prices related to the experimental determinations are very substantial; however, these costs can be reduced by using the QSPR modeling research. It is mostly utilized to investigate biological processes in addition to the various facets related to the structures, which is favorable for analyzing how a medicine molecule’s structural components affect its biological actions. With the aid of QSPR and QSAR techniques, models that can precisely predict the characteristics or actions of organic molecules can be built [13, 10, 8]. However, in order to formulate realistic models, a approach that is simultaneously skilled and effective of encoding the structures with predicted molecular structure descriptors is essential. When creating models, with the help of descriptors might equip an opportunity to zero down on particular traits that account for the activity or property of interest in the compounds [23, 17].

2. Materials and Analytical Techniques

In this research, we implemented a detailed methodology to calculate Sombor invariants and create Quantitative Structure-Property Relationship (QSPR) modeling for the molecular structures of various NSAID drugs, as shown in Figure 1. First, we assembled a exhaustive database of NSAID drugs, specifically Ketorolac, Meloxicam, Ibuprofen, Diclofenac, Nabumetone, Indomethacin, Naproxen, Etodolac, Piroxicam and Famotidine from trustworthy original sources (Table 1) and performed meticulous data preprocessing. Using established mathematical methods, particularly the edge partition technique, we calculated the Sombor indices with the help of Maple software, resulting in a set of descriptors. The dataset was then divided into subsets for testing, validation, and training in order to aid in the creation and assessment of models. The QSPR models were built using regression approach with specified algorithms and executed with SPSS software. To verify the generalizability of the models, we conducted external validation using an independent dataset. Our process included a detailed interpretation of model results and comprehensive statistical analysis. To ensure reproducibility, we provided access to the code and data. This meticulous approach ensures the durability of our QSPR models based on Sombor indices for NSAID drugs, focusing on chemical stability such as boiling point (BP), refractivity (R), complexity (C), polarity (Pol), and molecular weight (MW).

Drugs	Bp	R	Pol	C	MV	MW
Ketorolac	493.2	70.19	26.67	376	198.2	83.1
Naproxen	403.9	64.85	24.81	277	195.3	72.1
Meloxicam	581.3	88.62	34.25	628	220.7	83.5
Indomethacin	499.4	94.81	36.64	506	275.6	83.3
Etodolac	507.9	80.46	31.66	400	248.3	84.9
Diclofenac	412	75.46	27.93	304	209.8	73.1
Ibuprofen	157	60.73	23.76	203	203.3	62.4
Nabumetone	372.3	68.43	26.17	262	213.5	64.3
Famotidine	662.4	80.46	31.66	469	191.7	100.3
Piroxicam	568.5	87.04	32.27	611	229.8	91.3

Table 1. Several NSAIDs and associated physical and chemical characteristics

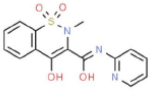
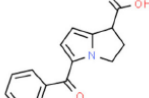
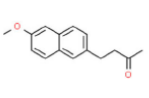
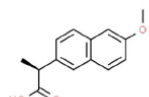
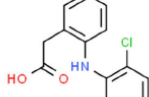
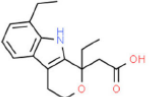
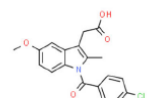
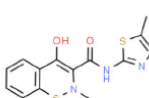
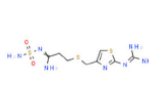
Piroxicam		Ketorolac		Nabumetone	
Molecular Structure	Properties	Molecular Structure	Properties	Molecular Structure	Properties
	Molecular Formula C ₁₉ H ₁₃ N ₃ O ₄ S Average mass 331.346 Da Monoisotopic mass 331.062683 Da ChemSpider ID 10442653		Molecular Formula C ₁₆ H ₁₃ NO ₃ Average mass 255.269 Da Monoisotopic mass 255.089539 Da ChemSpider ID 3694		Molecular Formula C ₁₆ H ₁₆ O ₂ Average mass 228.286 Da Monoisotopic mass 228.115036 Da ChemSpider ID 4256
Naproxen		Diclofenac		Etodolac	
Molecular Structure	Properties	Molecular Structure	Properties	Molecular Structure	Properties
	Molecular Formula C ₁₄ H ₁₄ O ₃ Average mass 230.259 Da Monoisotopic mass 230.094299 Da ChemSpider ID 137720		Molecular Formula C ₁₄ H ₁₁ Cl ₂ NO ₂ Average mass 296.149 Da Monoisotopic mass 295.016693 Da ChemSpider ID 2925		Molecular Formula C ₁₇ H ₂₁ NO ₃ Average mass 287.353 Da Monoisotopic mass 287.152130 Da ChemSpider ID 3192
Indometacin		Meloxicam		Famotidine	
Molecular Structure	Properties	Molecular Structure	Properties	Molecular Structure	Properties
	Molecular Formula C ₁₉ H ₁₆ ClNO ₄ Average mass 357.788 Da Monoisotopic mass 357.076782 Da ChemSpider ID 3584		Molecular Formula C ₁₄ H ₁₃ N ₃ O ₄ S ₂ Average mass 351.401 Da Monoisotopic mass 351.034760 Da ChemSpider ID 10442740		Molecular Formula C ₈ H ₁₂ N ₄ r ₇ O ₂ S ₃ Average mass 337.445 Da Monoisotopic mass 337.044922 Da ChemSpider ID 3208

Fig. 1. Graphical representation of NASID

3. Graph Invariants and Computational Results

Many graph invariants based on degrees, often referred to as 'topological indices,' have been introduced and extensively studied in both mathematical as well as in other related fields [23, 17].

$$TI(G) = \sum_{ij \in E(G)} F(d_i, d_j). \quad (1)$$

Here, $F(a, b)$ is expressing a commutative function with attribute i, e $F(a, b) = F(b, a)$ Sombor and its reduced version [7] are

$$SO(G) = \sum_{ij \in E(G)} \sqrt{d_i^2 + d_j^2}, \quad (2)$$

$$SO_{red}(G) = \sum_{uv \in E(G)} \sqrt{(d_i - 1)^2 + (d_j - 1)^2}. \quad (3)$$

Modified Sombor is represented by Kulli and Gutman [12], as follow

$$mSO_{red}(G) = \sum_{uv \in E(G)} \frac{1}{\sqrt{d_i^2 + d_j^2}}.$$

Max and min Sombor invariants were presented by Mendez-Bermudez et al. in [14]

$$maxSO(G) = \sum_{ij \in E(G)} \max(d_i, d_j),$$

$$minSO(G) = \sum_{ij \in E(G)} \min(d_i, d_j).$$

Table 2 lists all the calculated values of NSAID for various types of Sombor invariants. Figures 2 and 3 show two and three dimensional representations of the computed topological indices for different NSAID.

Chemical Compounds	SO	SO_{red}	mSO	$maxSO$	$minSO$
Ketorolac	73.53	44.87	6.148	57	45
Ibuprofen	48.48	28.61	4.73	27	39
Diclofenac	68.36	41.44	5.95	55	39
Meloxicam	92.2	58.90	6.96	75	51
Nabumetone	56.08	32.85	5.32	45	33
Naproxen	62.55	38.43	5.30	51	35
Indomethacin	95.89	59.64	7.79	77	55
Etodolac	82.99	53.39	5.26	68	46
Piroxicam	73.40	56.67	7.15	72	52
Famotidine	70.09	43.94	5.81	60	34

Table 2. Topological invariants of NSAID.

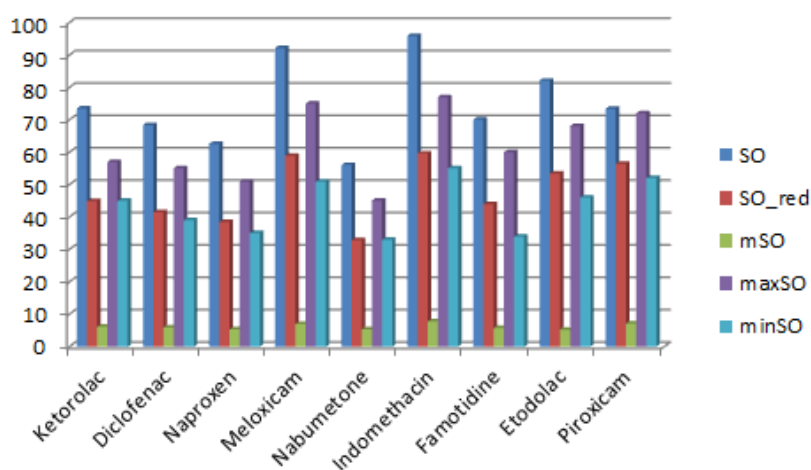


Fig. 2. 3D representation of NSAID via Sombor invariants

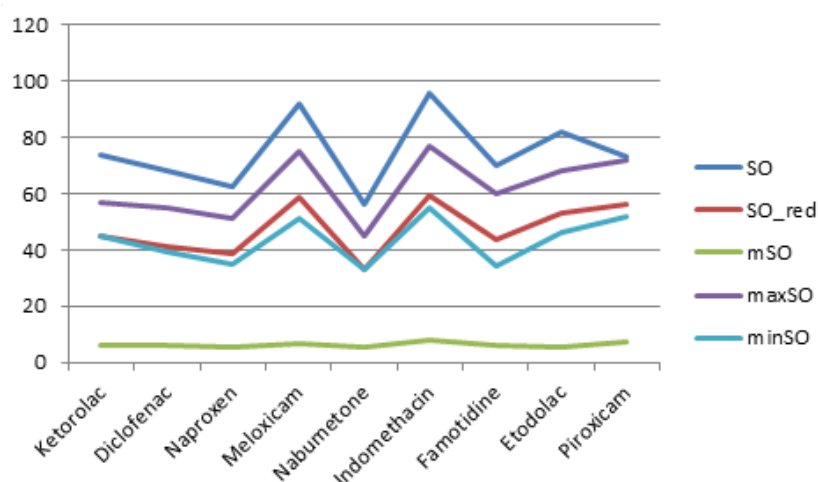


Fig. 3. 2D representation of NSAID via Sombor invariants

Table 2, represents the values of Sombor index (SO), reduce Sombor version (SO_{red}), modified Sombor (mSO), maximum version of Sombor ($maxSO$) and minimum Sombor version ($minSO$),

for above mentioned NSAIDs drugs. Figures 2 and 3, represents 2 and 3 dimensional graphical representations of nine NSAIDs.

4. Regression Model and Structure Analysis

Regression models (RMs) are statistical methods employed to examine and illustrate the association between a dependent variable and one or more independent variables [24]. Typical RMs consist of linear RM, logistic RM, and polynomial RM, each appropriate for different data types and research questions. In this study, we will employ a linear regression model, as represented by equation 4, to investigate the bonds between TIs and the physiochemical characteristics of NSAIDs.

$$P = \alpha + \beta(TI). \quad (4)$$

NSAID's characteristic are represented by C. TI is refer as independent variable, two regression confident are a and b, we will use SPSS to find these constants. A five TIs for NSAID and their attributes are analyzed using a linear regression model.

This section comprises of five subsections. Subsection 4.1, represents the linear regression model of Sombor index with different physicochemical properties of NSAIDs drugs. Similarly, Subsections 4.2 - 4.5, are for reduce, modified, maximum and minimum Sombor indices, respectively.

4.1. Regression models for SO

$$\begin{aligned} BP &= 6.416(SO) + 1.480, \\ POL &= 0.266(SO) + 10.803, \\ C &= 7.734(SO) - 156.10, \\ R &= 0.660(SO) + 29.043, \\ MW &= 0.471(SO)45.776, \\ MV &= 1.482(SO) + 116.383. \end{aligned}$$

4.2. Regression models for SO_{red}

$$\begin{aligned} BP &= 9.476(SO_{red}) + 31.066, \\ POL &= 0.361(SO_{red}) + 13.043, \\ C &= 12.166(SO_{red}) - 154.500, \\ R &= 0.945(SO_{red}) + 33.736, \\ MW &= 0.746(SO_{red}) + 45.621, \\ MV &= 1.641(SO_{red}) + 143.342. \end{aligned}$$

4.3. Regression models for *mSO*

$$\begin{aligned}
 BP &= 84.433(mSO) - 44.356, \\
 POL &= 3.5997(mSO) + 7.832, \\
 C &= 124.118(mSO) - 346.319, \\
 R &= 9.924(mSO) + 17.141, \\
 MW &= 6.301(mSO) + 41.759, \\
 MV &= 11.336(mSO) + 155.129.
 \end{aligned}$$

4.4. Regression models for *maxSO*

$$\begin{aligned}
 BP &= 7.5955(maxSO) + 76.044, \\
 POL &= 0.207(maxSO) + 14.796, \\
 C &= 8.4489(maxSO) - 92.3505, \\
 R &= 0.6698(maxSO) + 37.7846, \\
 MW &= 0.5594(maxSO) + 46.9939, \\
 MV &= 1.2811(maxSO) + 148.4177.
 \end{aligned}$$

4.5. Regression models for *minSO*

$$\begin{aligned}
 BP &= 6.1216(minSO) + 203.1737, \\
 POL &= 0.3975(minSO) + 12.5278, \\
 C &= 13.5871(minSO) - 179.2887, \\
 R &= 1.0657(minSO) + 31.3886, \\
 MW &= 0.5623(minSO) + 55.7063, \\
 MV &= 106.4717(minSO) + 2.7307.
 \end{aligned}$$

5. Comparative Analysis of Predictive and Experimental Data

This section will discuss the comparison of experimental data to observed values derived from a well-designed linear regression model. Values for the variables being considered are projected by applying the predictive capability of the linear regression model. These projected values are then carefully compared with the experimental data to ascertain how accurate the model is. A custom Python application is developed to achieve this comparison and estimate the level of accuracy. This application is written with precision in calculating the percentage error between the experimental data and the expected values, which is indicative of how well the model captures the subtleties and underlying trends seen in the empirical data. This approach will help better our knowledge of the capabilities of statistical modeling techniques toward prediction power by identifying pros and cons in the linear regression model with regards to approximating occurrences in the real world by this systematic review.

5.1. Analysis of Ketorolac drug

This subsection compares the exact value of the drug ketorolac with the values calculated from a linear regression model from Sombor. An extensive Table 3 is shown which presents the comparison between the calculated and actual values. Moreover, the corresponding Figures 4-9 illustrate the accuracy of each value (B.P, Pol, C, R, MW, MV) along with their error, thus visually describing the accuracy and reliability of the measurements.

Property	Exact Value	Observed values				
		SO	SO_{red}	mSO	$maxSO$	$minSO$
B.P	493.2	473.21	456.25	474.91	436.11	478.65
Pol	26.67	29.92	29.24	29.97	28.60	30.42
C	376	412.66	391.39	417	373.08	432.13
R	70.19	77.58	76.14	78.17	74.52	79.35
MW	83.1	80.41	79.09	80.51	78.23	81.01
MV	198.2	225.37	216.97	224.85	218.22	229.35

Table 3. Actual and observed values of Ketorolac

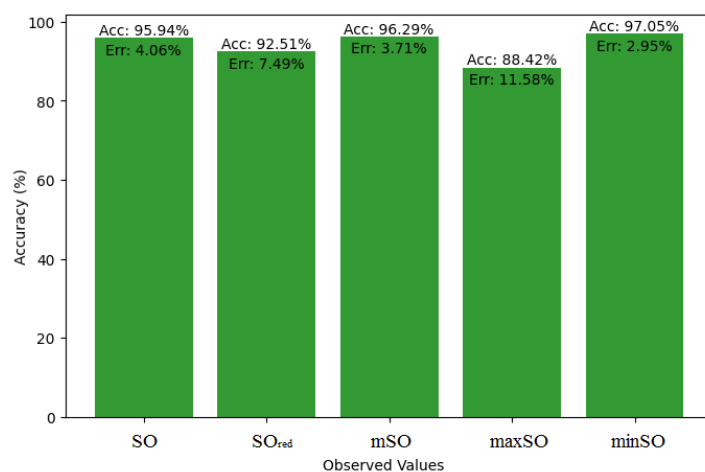


Fig. 4. Accuracy and error comparison for Ketorolac's B.P

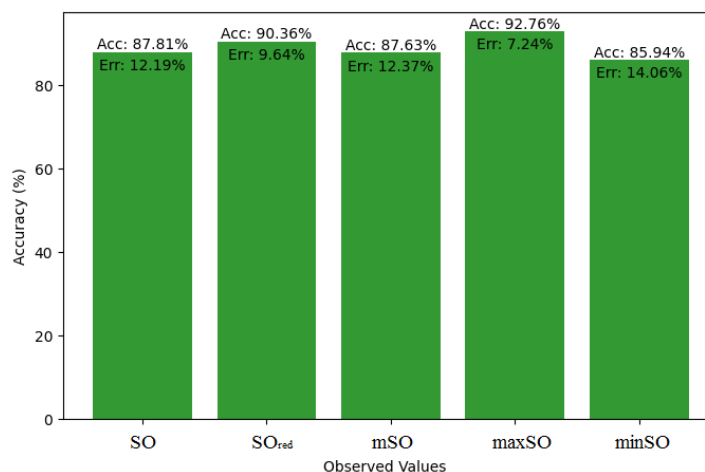


Fig. 5. Accuracy and error comparison for Ketorolac's Pol

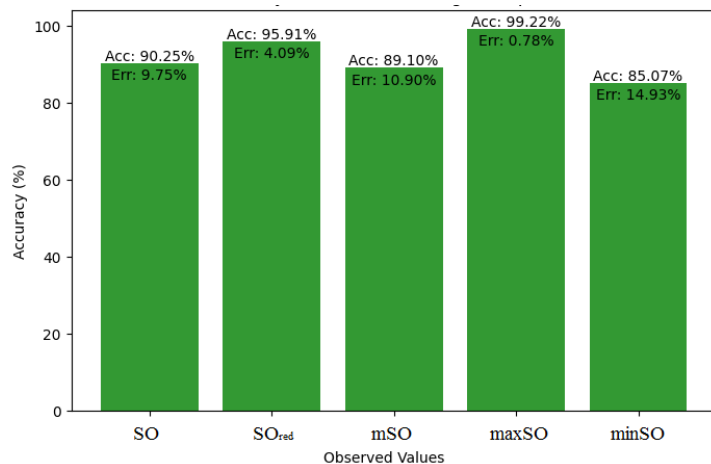


Fig. 6. Accuracy and error comparison for Ketorolac's C

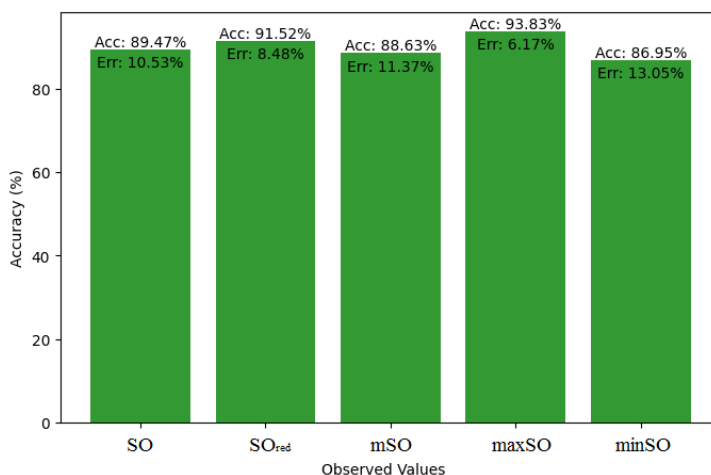


Fig. 7. Accuracy and error comparison for Ketorolac's R

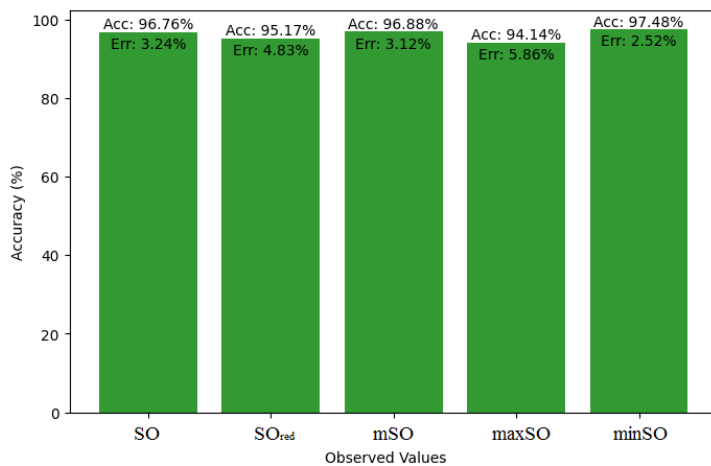


Fig. 8. Accuracy and error comparison for Ketorolac's MW

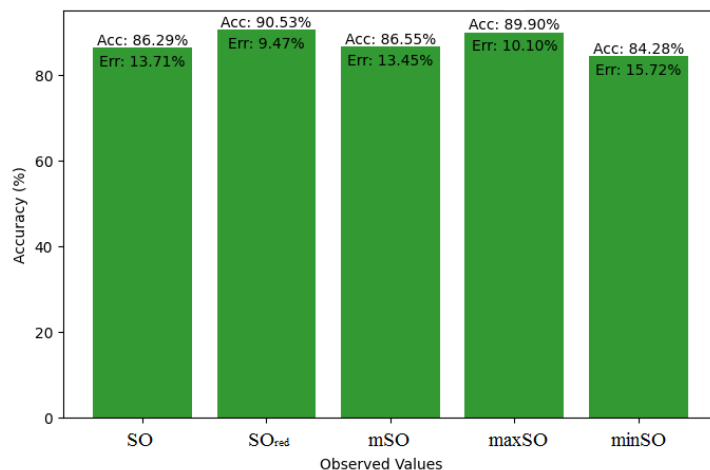


Fig. 9. Accuracy and error comparison for Ketorolac's MV

5.2. Analysis of diclofenac drug

Here, we initiate a comparative analysis between the actual value of Diclofenac drug and the noted values garnered from our algorithm. An informative Table 4 is designed, defining the alignment of the data points that are observed and real. There are companion graphs that show each value's accuracy alongside the associated inaccuracy, offering a visual representation of the reliability and fidelity of the measurements in Figures 10-15

Property	Exact Value	Observed values				
		SO	SO _{red}	mSO	maxSO	minSO
B.P	412	440.08	423.75	458.02	423.48	441.92
Pol	27.93	28.58	28	29.25	28.18	28.03
C	304	372.60	349.66	392.18	360.09	350.61
R	75.46	74.16	72.90	76.19	73.41	72.95
MW	73.1	77.97	76.54	79.25	77.53	77.64
MV	209.8	217.69	211.35	225.58	215.93	212.97

Table 4. Actual and observed values of diclofenac

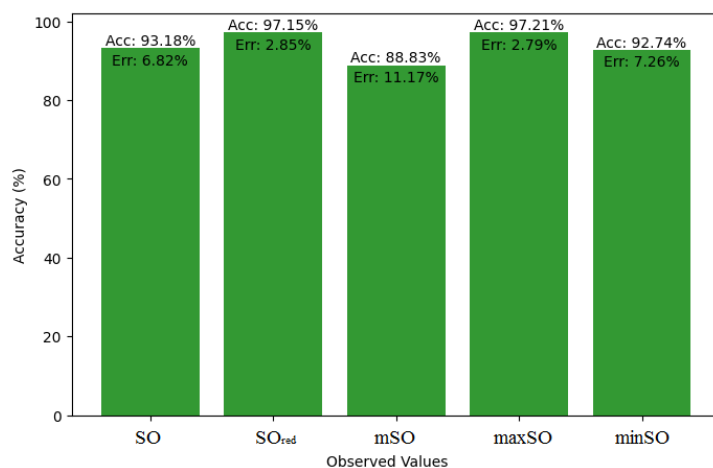


Fig. 10. Accuracy and error comparison for diclofenac's B.P

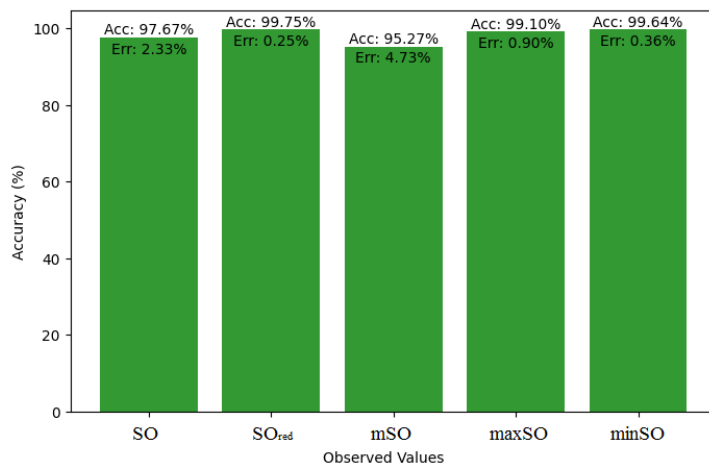


Fig. 11. Accuracy and error comparison for diclofenac's Pol

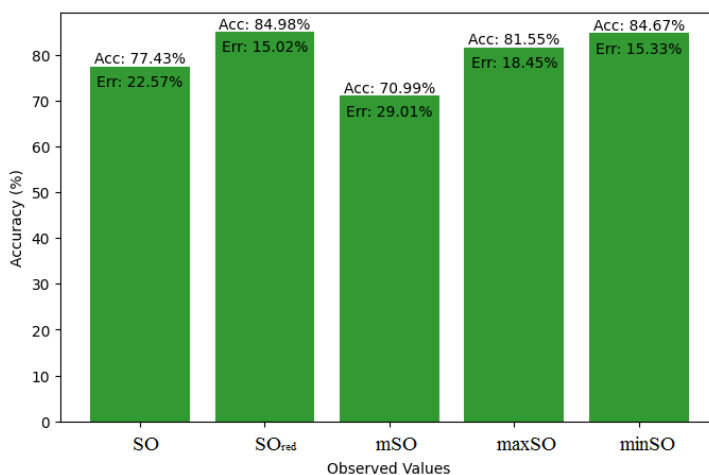


Fig. 12. Accuracy and error comparison for diclofenac's C

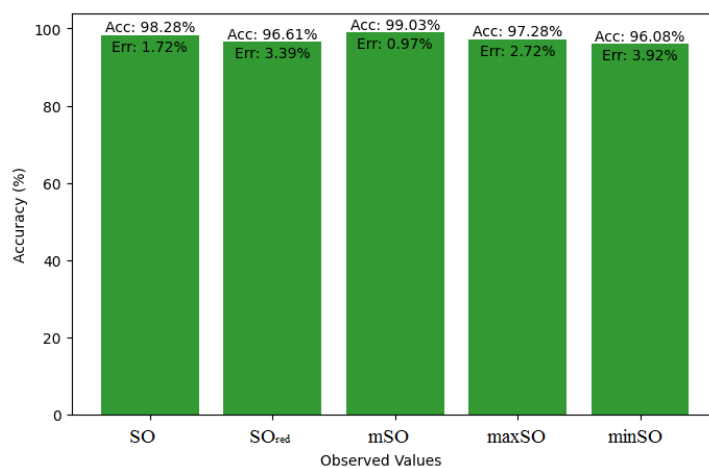


Fig. 13. Accuracy and error comparison for diclofenac's R

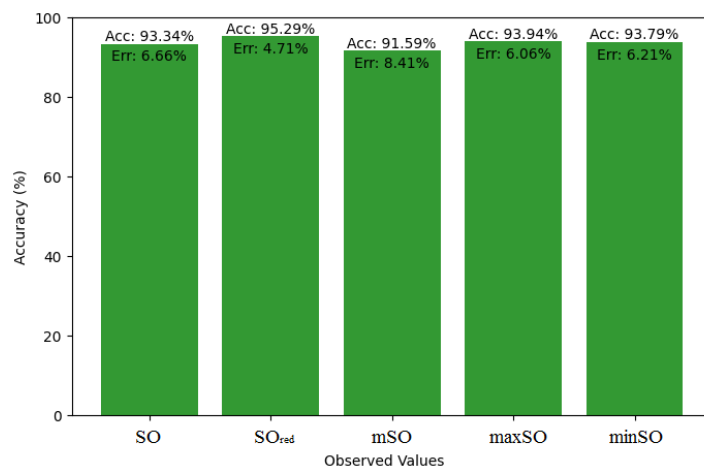


Fig. 14. Accuracy and error comparison for diclofenac's MW

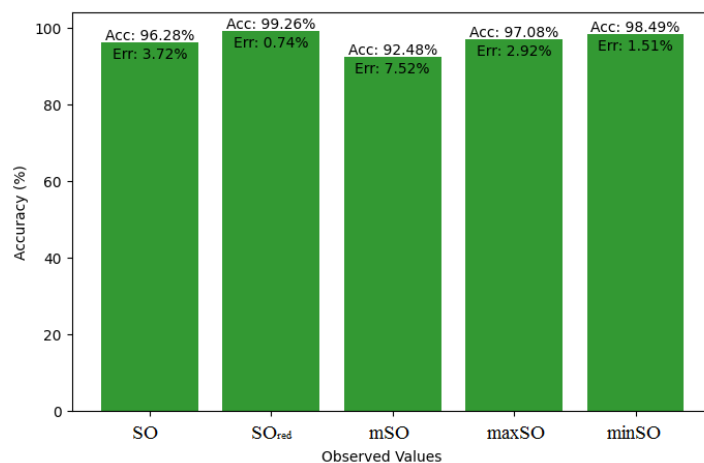


Fig. 15. Accuracy and error comparison for diclofenac's MV

5.3. Analysis of naproxen drug

This section presents a comparison study of the exact value of Naproxen Drug and the observable values that come from sombor based linear regression model. A detailed Table 5 that shows the comparison of observed and real values is provided. In addition, Figures 16-21 that explain each value's accuracy and associated error are included, providing a visual depiction of the measurements' dependability and consistency.

Property	Exact Value	Observed values				
		SO	SO _{red}	mSO	maxSO	minSO
B.P	403.9	402.80	395.23	403.14	398.21	417.43
Pol	24.81	27.07	26.92	26.91	27.35	26.44
C	277	327.66	313.04	312.51	334.11	296.26
R	64.85	70.33	70.05	69.74	71.21	68.68
MW	72.1	75.24	74.29	75.15	76.165	75.38
MV	195.3	209.08	206.41	215.21	211.35	202.04

Table 5. Actual and Observed values of Naproxen

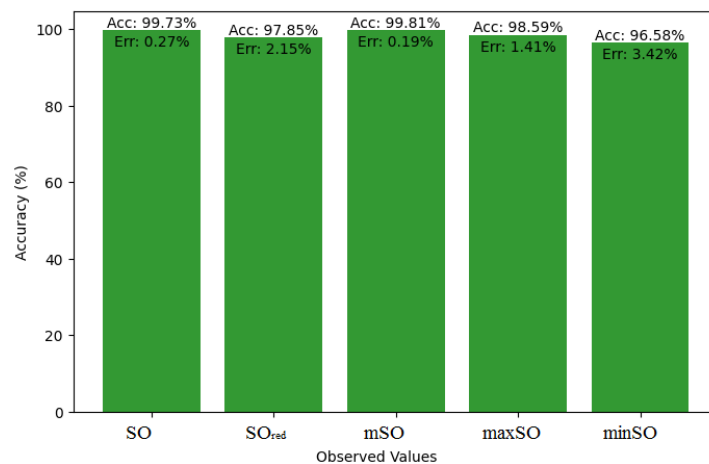


Fig. 16. Accuracy and error comparison for naproxen's B.P

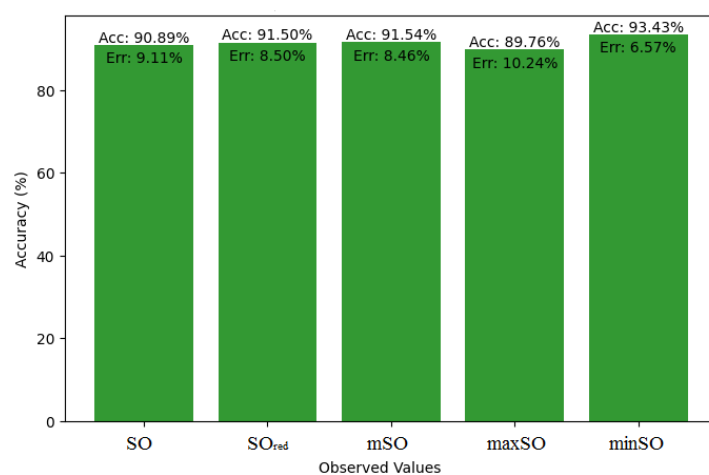


Fig. 17. Accuracy and error comparison for naproxen's Pol

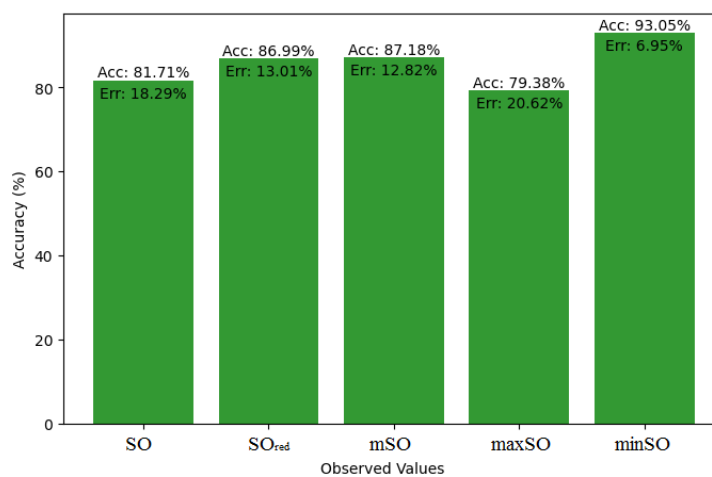


Fig. 18. Accuracy and error comparison for naproxen's C

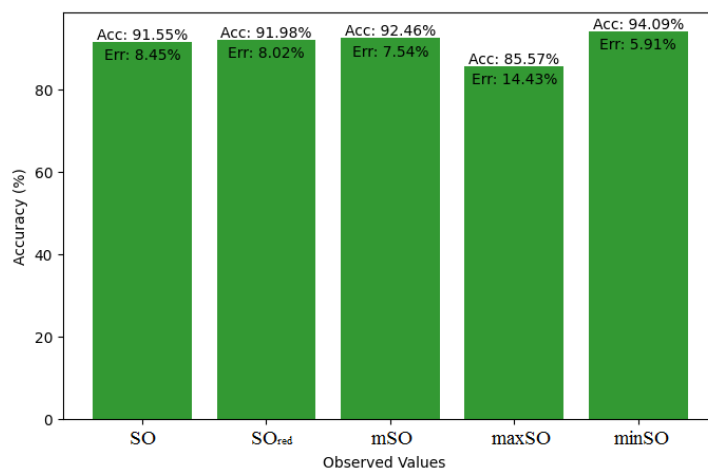


Fig. 19. Accuracy and error comparison for naproxen's R

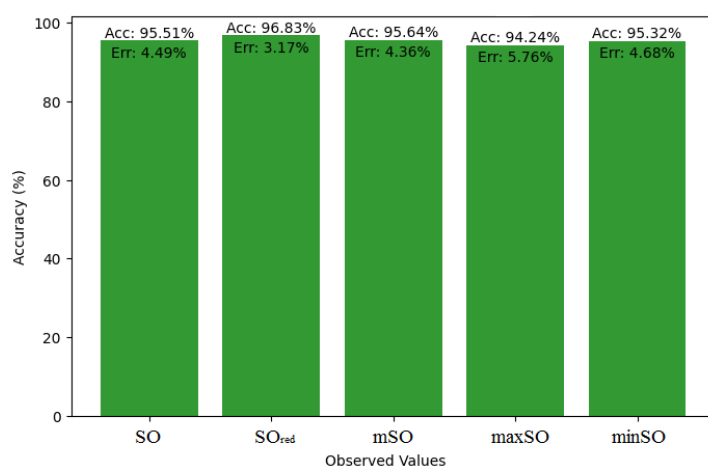


Fig. 20. Accuracy and error comparison for naproxen's MW

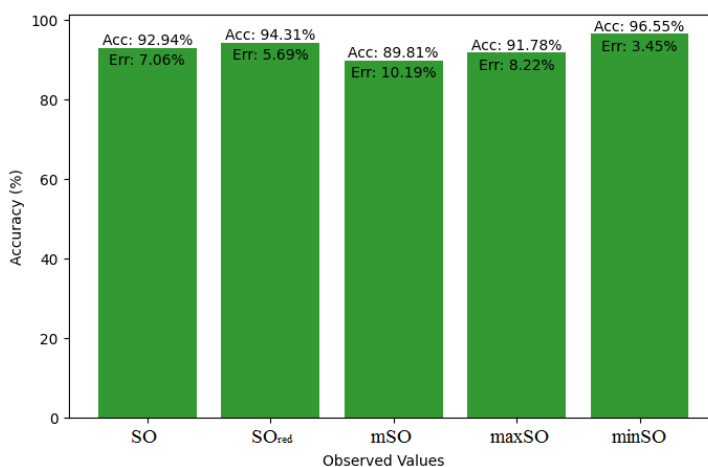


Fig. 21. Accuracy and error comparison for naproxen's MV

5.4. Analysis of meloxicam drug

In this subsection, we compare the exact value of the drug Meloxicam with the observed values that were discovered with the help of Smbor indices and linear regression model. Table 6, illustrates the

alignment of observed and real data points is created. Furthermore, complimentary graphs 22-27 are supplied to illustrate the precision and accuracy of each result in conjunction with the associated error, allowing for a thorough comprehension of the measures' dependability and accuracy.

Property	Exact Value	Observed values				
		SO	SO_{red}	mSO	maxSO	minSO
B.P	581.3	593.48	589.20	543.30	549.82	515.38
Pol	34.25	34.79	34.31	32.89	32.321	32.80
C	628	557.52	562.08	517.54	489.99	513.65
R	88.62	89.94	89.40	86.21	83.43	83.45
MW	83.5	89.24	89.44	85.61	84.39	84.38
MV	220.7	253.13	239.50	234.03	238.83	245.74

Table 6. Actual and observed values of meloxican

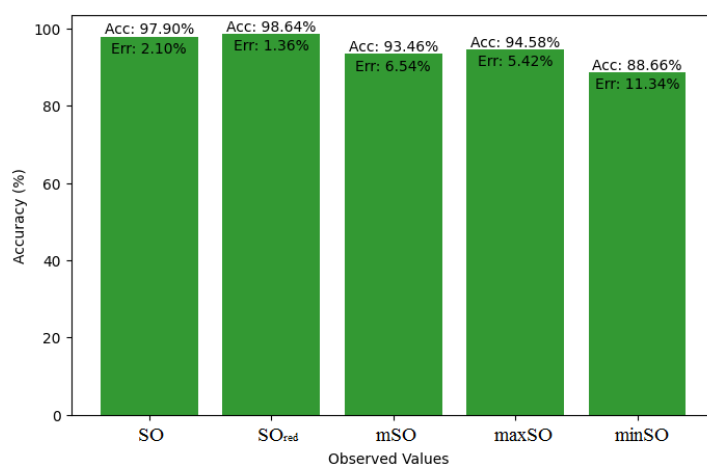


Fig. 22. Accuracy and error comparison for meloxican's B.P

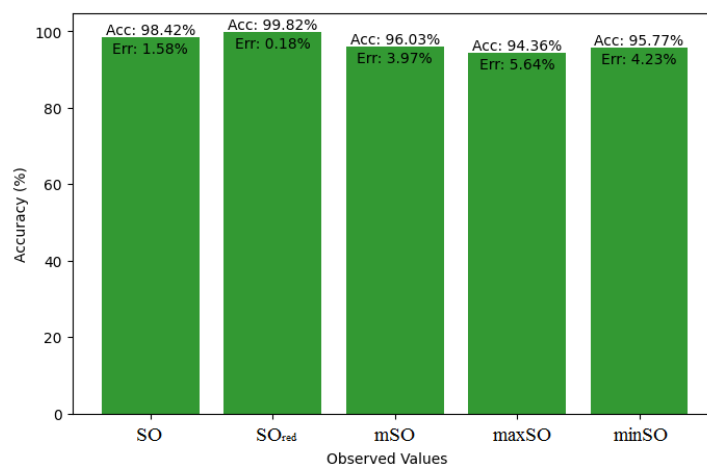


Fig. 23. Accuracy and error comparison for meloxican's Pol

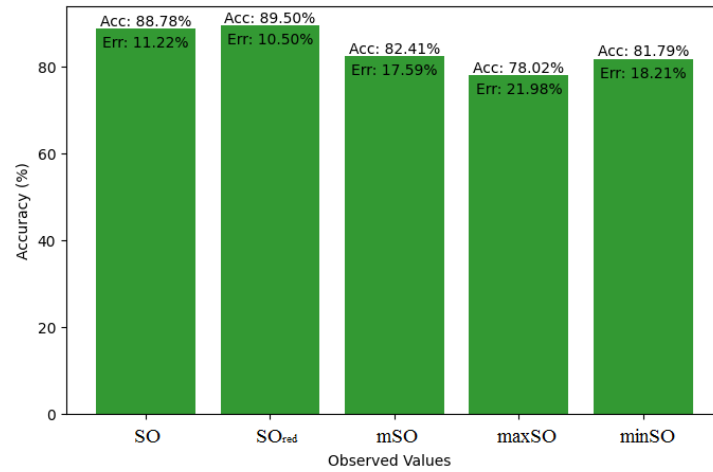


Fig. 24. Accuracy and error comparison for meloxican's C

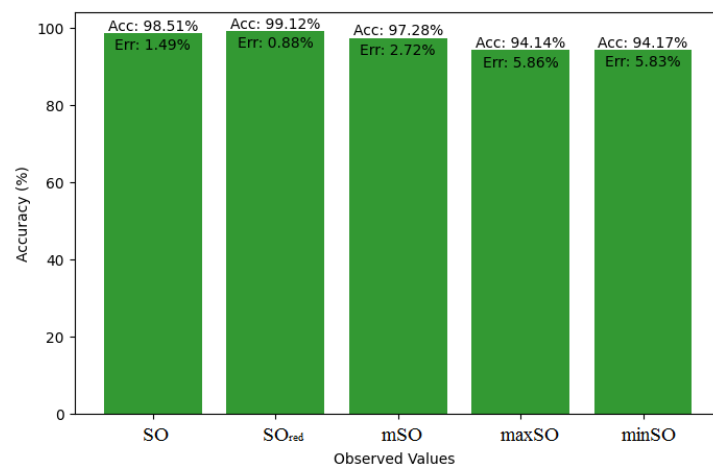


Fig. 25. Accuracy and error comparison for meloxican's R

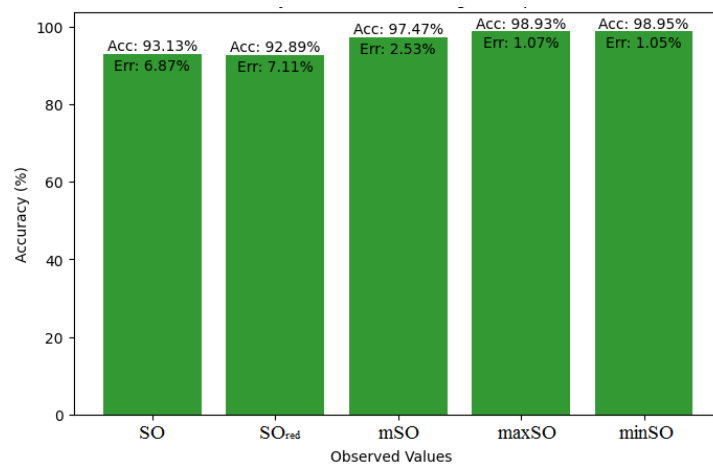


Fig. 26. Accuracy and error comparison for meloxican's MW

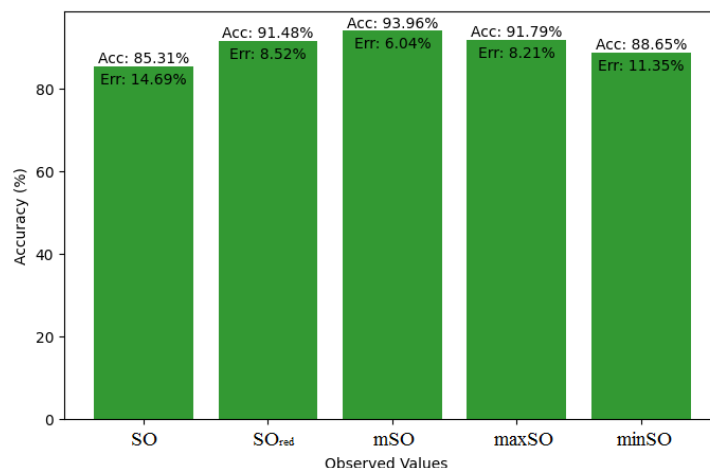


Fig. 27. Accuracy and error comparison for meloxicam's MV

5.5. Analysis of nabumetone drug

We compare the exact value of the medication naproxenone with the observed values derived from empirical analysis in this subsection. A comprehensive Table 7 is created, showing the agreement between observed and real data points. Furthermore, graphical depictions 28-33 are incorporated to illustrate the precision of every number in conjunction with its associated error, providing valuable perspectives on the dependability and uniformity of the measurements.

Property	Exact Value	Observed values				
		SO	SO _{red}	mSO	maxSO	minSO
B.P	372.3	361.29	342.35	404.83	360.31	405.19
Pol	26.17	25.38	24.90	26.98	27.35	25.65
C	262	277.62	245.15	313.99	334.11	269.09
R	68.43	66.06	64.78	69.94	71.21	66.56
MW	64.3	72.19	70.13	75.28	76.16	74.26
MV	213.5	199.49	197.25	215.44	211.35	196.58

Table 7. Actual and observed values of nabumetone

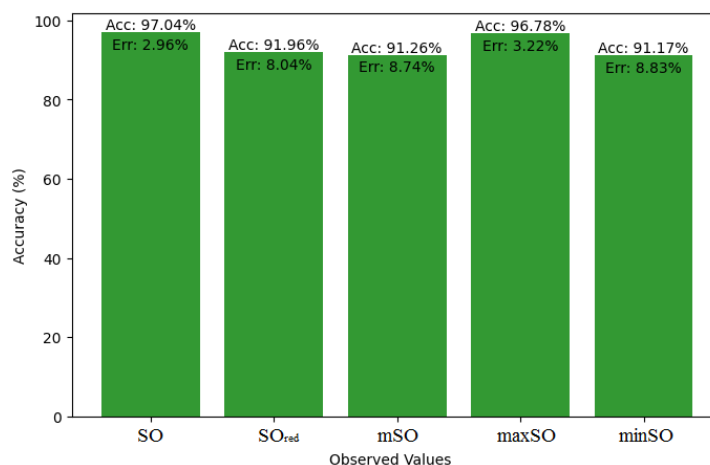


Fig. 28. Accuracy and error comparison for nabumetone's B.P

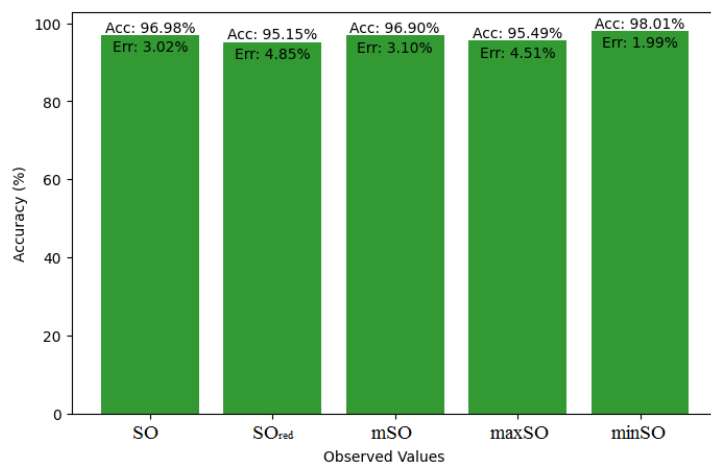


Fig. 29. Accuracy and error comparison for nabumetone's Pol

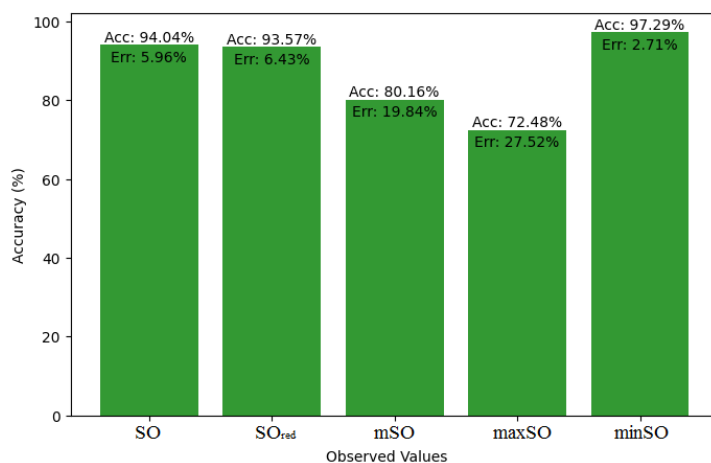


Fig. 30. Accuracy and error comparison for nabumetone's C

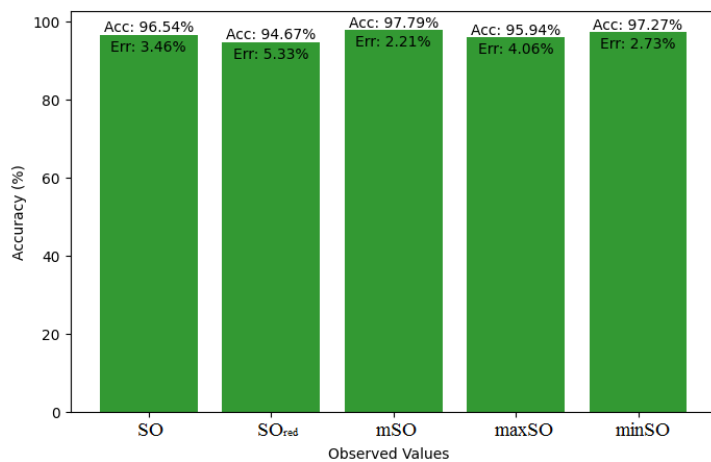


Fig. 31. Accuracy and error comparison for nabumetone's R

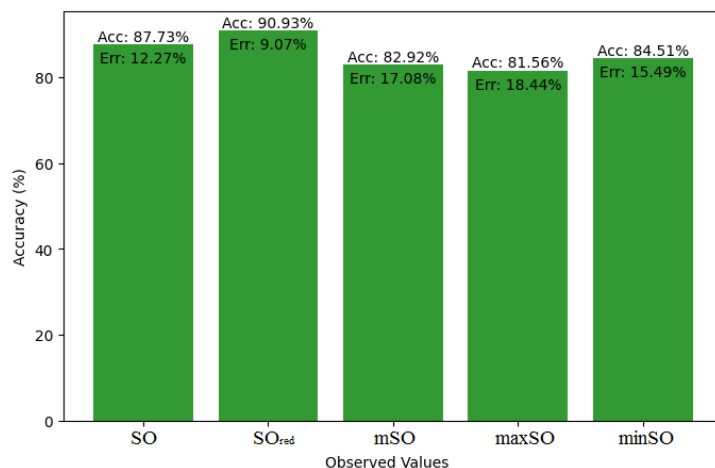


Fig. 32. Accuracy and error comparison for nabumetone's MW

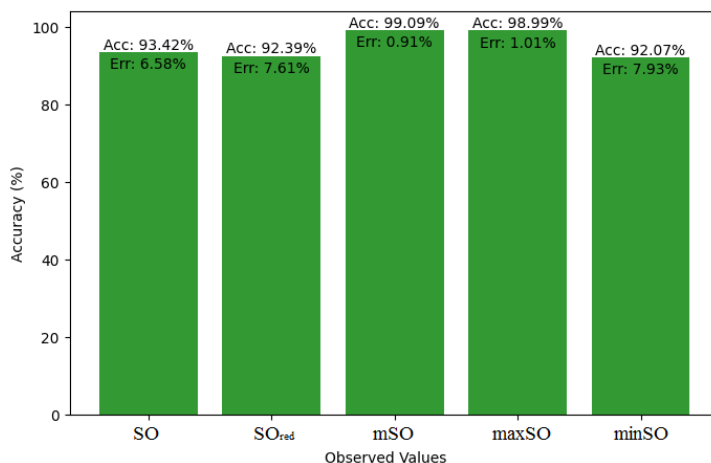


Fig. 33. Accuracy and error comparison for nabumetone's MV

5.6. Analysis of indomethacin drug

Here, we will compare the exact value of the medication indomethacin with the observed values obtained from empirical research in this subsection. A detailed Table 8 is shown that shows how the observed and real data points line up. In addition, graphs 34-39 that show each value's accuracy and related error are included, providing a visual depiction of the measures' dependability and precision.

Property	Exact Value	Observed values				
		SO	SO _{red}	mSO	maxSO	minSO
B.P	499.4	616.71	596.21	613.38	562.45	539.86
Pol	36.4	35.73	34.57	35.87	32.74	34.39
C	506	585.51	571.08	620.56	502.98	568
R	94.81	125.59	90.10	94.45	85.34	90
MW	83.3	90.94	90.11	90.84	85.08	86.63
MV	275.6	258.49	241.21	243.44	241.12	256,66

Table 8. Actual and observed values of indomethacin

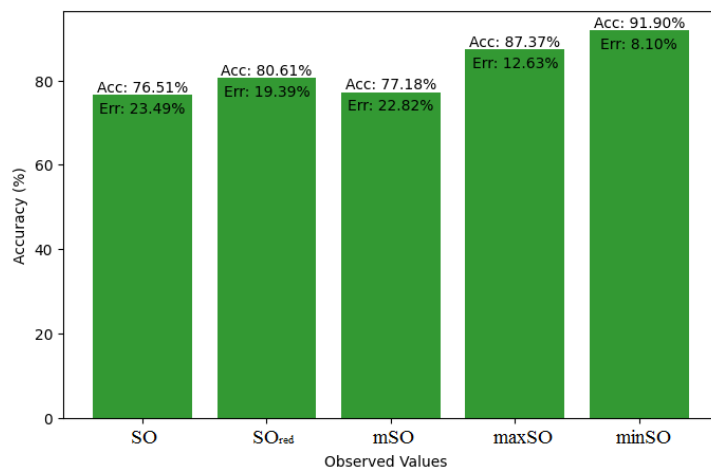


Fig. 34. Accuracy and error comparison for indomethanic's B.P

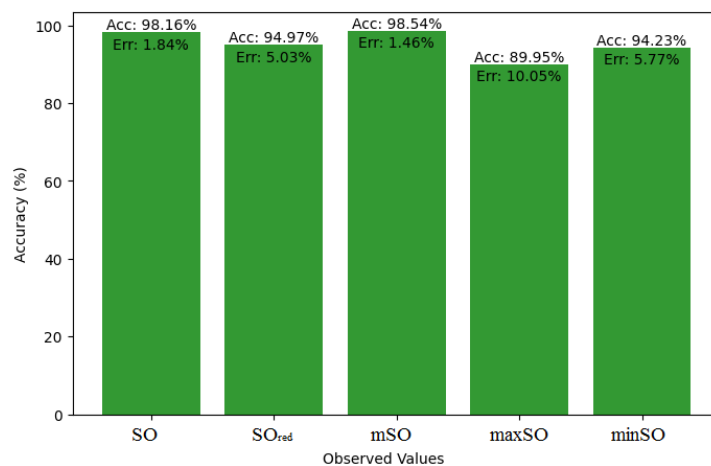


Fig. 35. Accuracy and error comparison for indomethanic's Pol

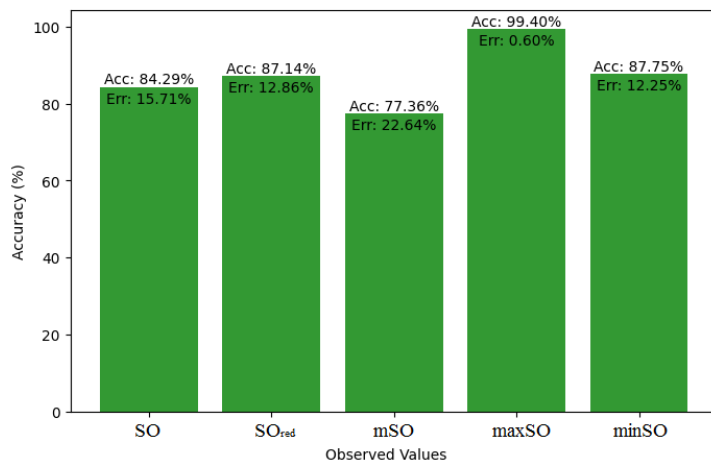


Fig. 36. Accuracy and error comparison for indomethanic's C

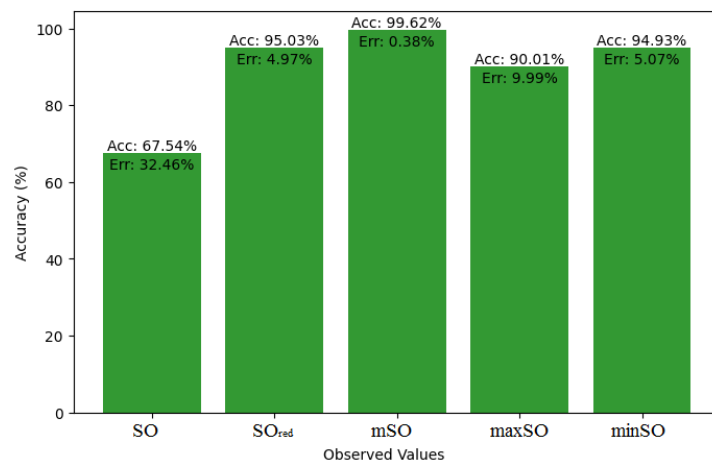


Fig. 37. Accuracy and error comparison for indomethacin's R

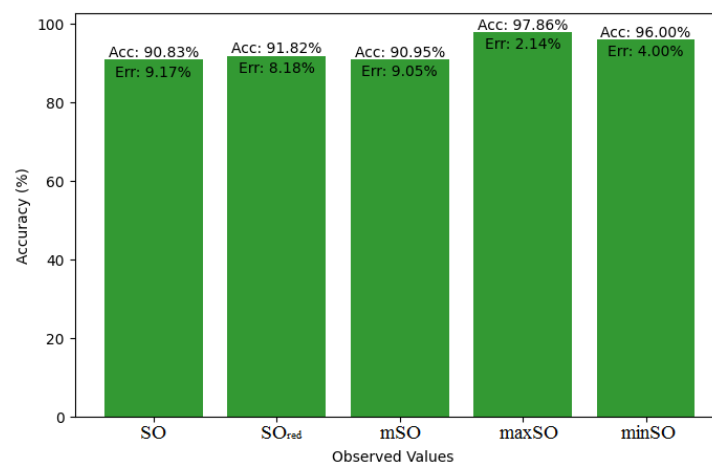


Fig. 38. Accuracy and error comparison for indomethacin's MW

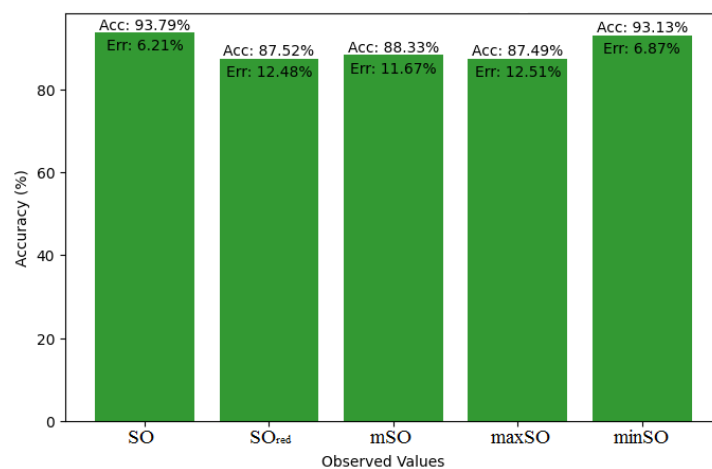


Fig. 39. Accuracy and error comparison for indomethacin's MV

5.7. Analysis of famotidine Drug

This subsection compares the exact value of the medication famotidine with the observed values with the help of linear regression model. A comprehensive Table 9 is created, showing the alliance between

observed and real data points. Moreover, Figures 40-45 are included to demonstrate the precision and accuracy of every result in conjunction with the corresponding error percentage, so enabling a thorough comprehension of the dependability and accuracy of the measurements.

Property	Exact Value	Observed values				
		SO	SO_{red}	mSO	maxSO	minSO
B.P	662.4	451.18	447.44	446.20	455.06	411.31
Pol	31.66	29.03	28.91	28.75	29.22	26.04
C	469	385.98	380.07	374.81	392.57	282.67
R	80.46	75.30	75.26	74.80	76.17	67.62
MW	100.3	78.79	78.40	78.37	79.25	74.82
MV	191.7	220.26	215.45	221	221.65	199.32

Table 9. Actual and observed values of famotidine

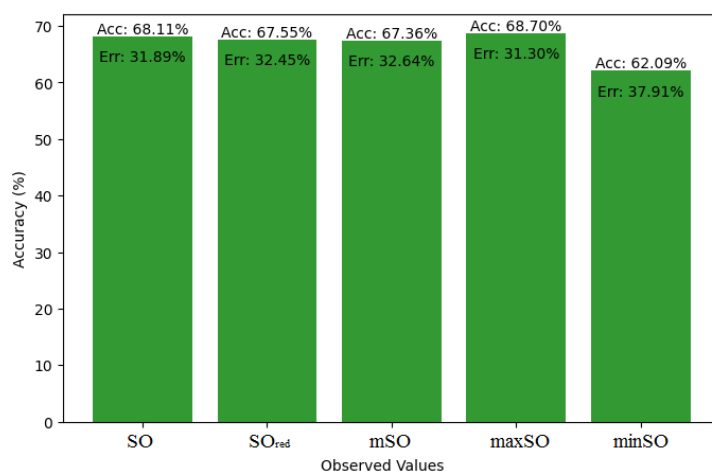


Fig. 40. Accuracy and error comparison for famotidine's B.P

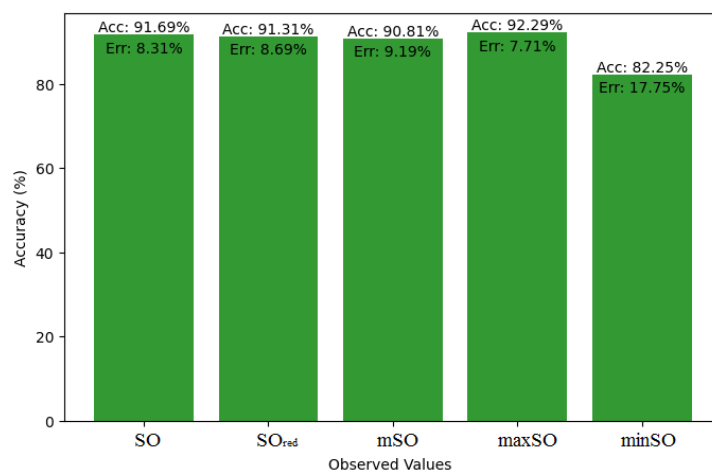


Fig. 41. Accuracy and error comparison for famotidine's Pol

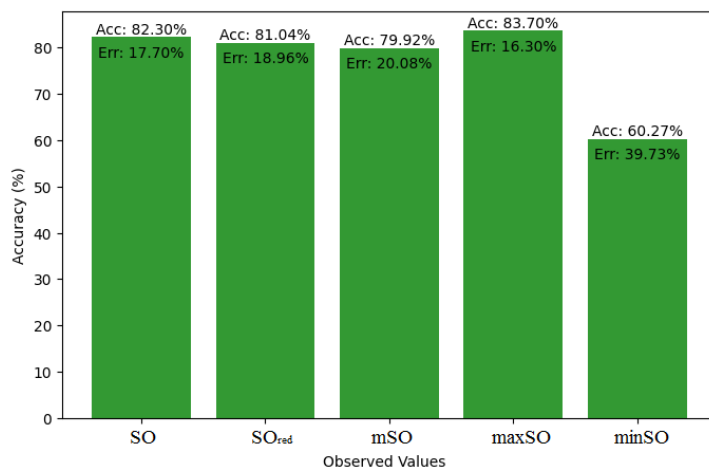


Fig. 42. Accuracy and error comparison for famotidine's C

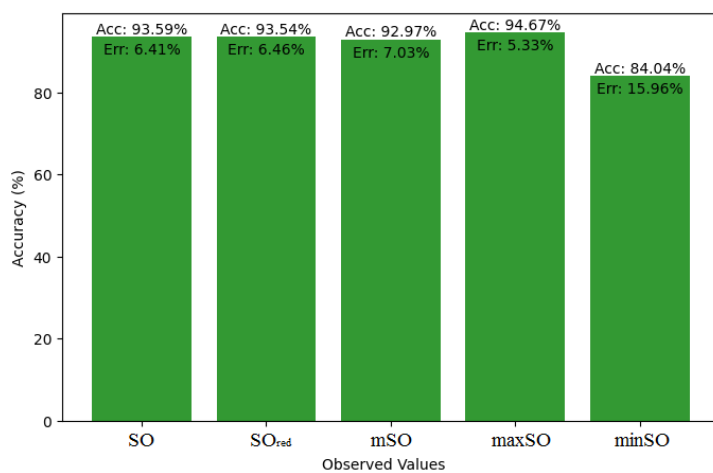


Fig. 43. Accuracy and error comparison for famotidine's R

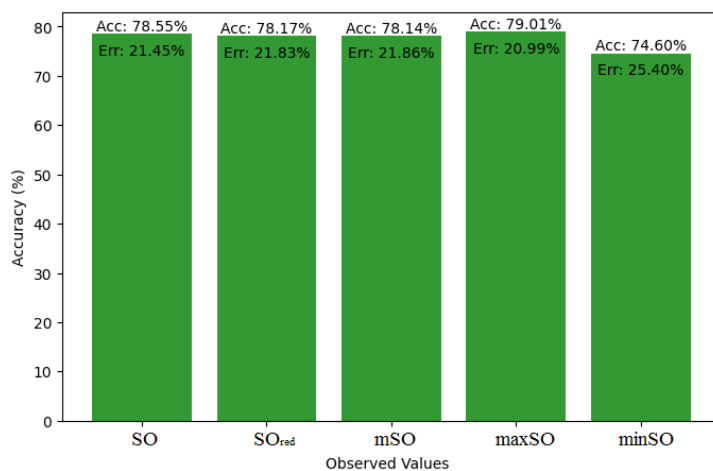


Fig. 44. Accuracy and error comparison for famotidine's MW

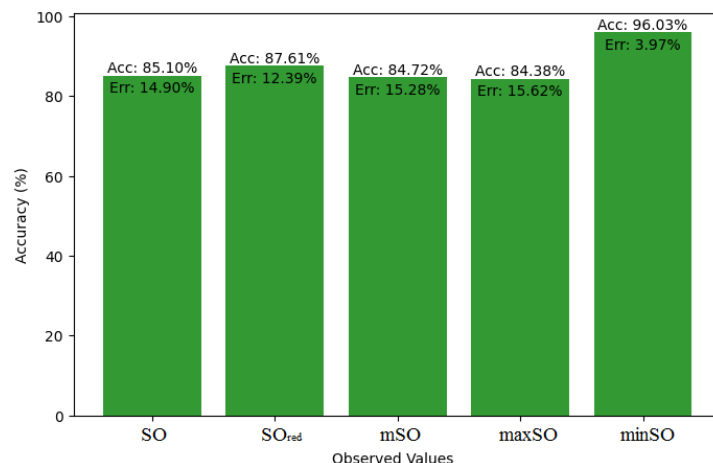


Fig. 45. Accuracy and error comparison for famotidine's MV

5.8. Analysis of etodolac drug

This subsection presents a comparative study between the exact value of the medication etodolac and the observed values derived from empirical research. A detailed table 10 that shows how the observed and real data points line up is provided. Furthermore, Figures 46-51 show each value's accuracy together with the corresponding error percentage are included, providing information about the consistency and dependability of the measurements.

Property	Exact Value	Observed values				
		SO	SO _{red}	mSO	maxSO	minSO
B.P	507.9	533.94	536.99	399.76	505.6	484.77
Pol	31.66	32.38	32.32	26.77	30.87	30.81
C	400	485.74	495.04	306.54	444.53	445.72
R	80.46	83.82	84.19	69.34	80.58	80.41
MW	84.9	84.86	85.45	74.90	81.99	81.57
MV	248.3	239.37	230.95	214.76	230.81	232.08

Table 10. Actual and observed values of etodolac

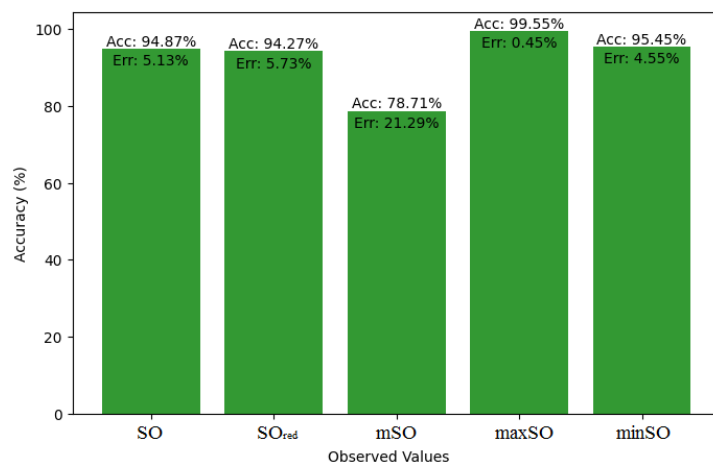


Fig. 46. Accuracy and error comparison for etodolac's B.P

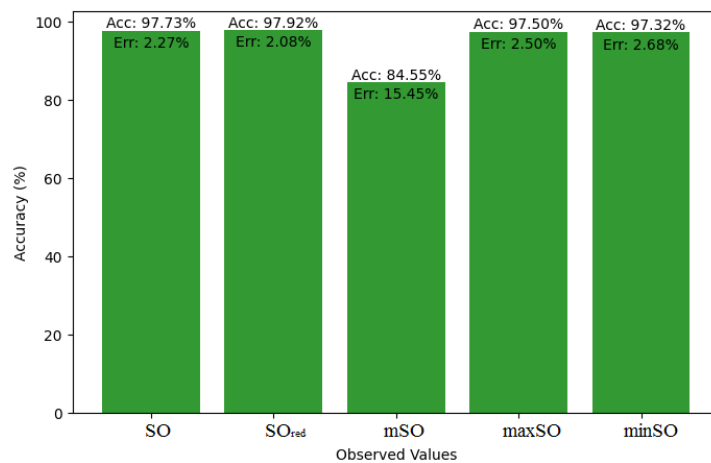


Fig. 47. Accuracy and error comparison for etodolac's Pol



Fig. 48. Accuracy and error comparison for etodolac's C

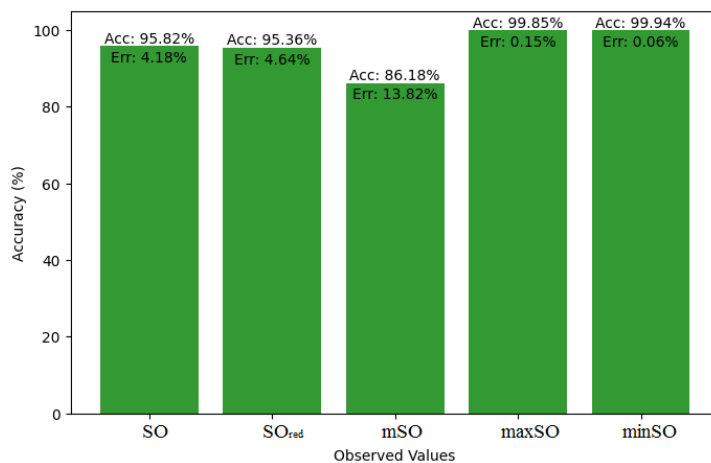


Fig. 49. Accuracy and error comparison for etodolac's R

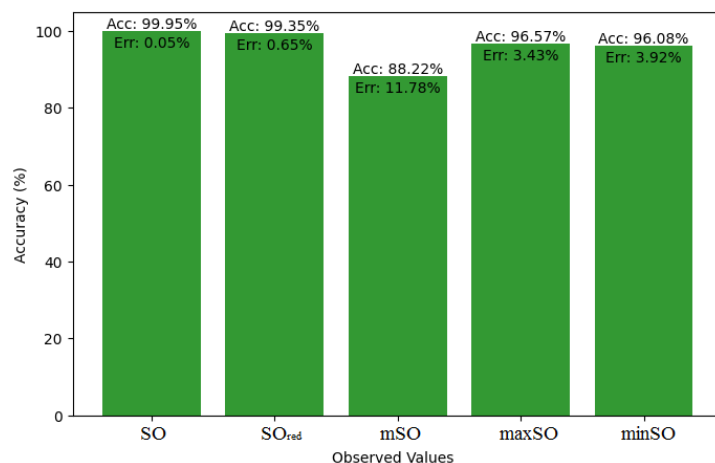


Fig. 50. Accuracy and error comparison for etodolac's MW

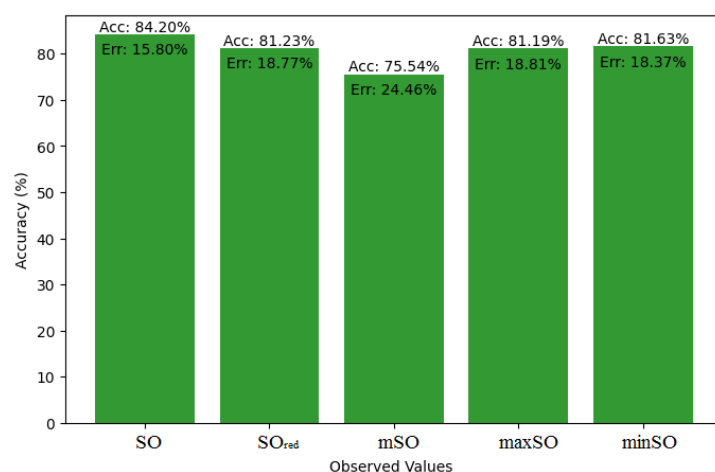


Fig. 51. Accuracy and error comparison for etodolac's MV

5.9. Analysis of piroxicam drug

We start a comparative analysis in this sub section between the theoretical value of Piroxicam Drug and the observed values obtained from empirical study. A detailed Table 11 is prepared, which shows the observed and actual data points alignment. Figures 52-57 give the correctness of each value with the corresponding error percentage, thereby giving a detailed assessment of the measures' reliability and accuracy.

Property	Exact Value	Observed values				
		SO	SO _{red}	mSO	maxSO	minSO
B.P	568.5	472.41	568.07	559.34	530.87	521.50
Pol	32.27	29.89	33.50	33.57	31.7	33.20
C	611	411.58	534.95	541.12	470.51	527.24
R	87.04	77.49	87.29	88.10	82.78	86.81
MW	91.3	80.35	87.90	86.81	83.36	84.85
MV	229.8	225.16	236.34	236.18	235.39	248.47

Table 11. Actual and observed values of piroxicam

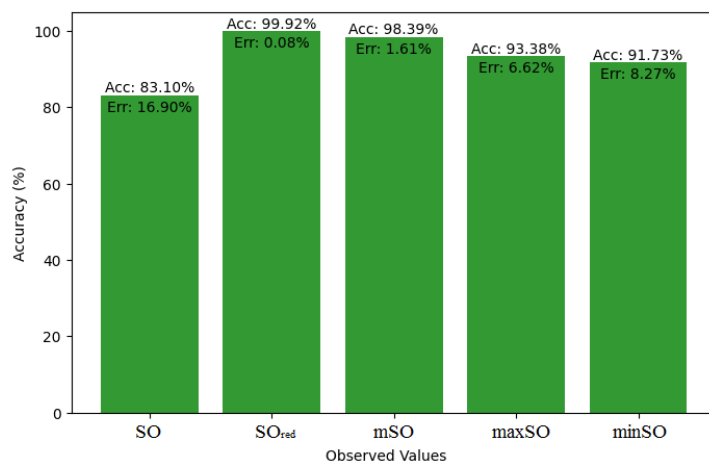


Fig. 52. Accuracy and error comparison for piroxicam's B.P

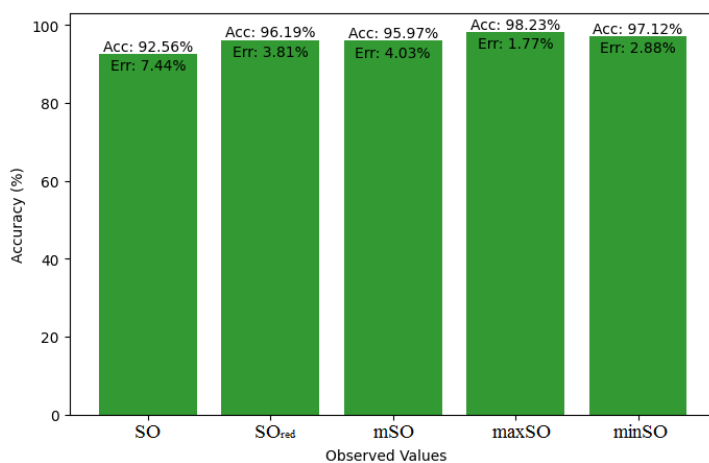


Fig. 53. Accuracy and error comparison for piroxicam's Pol



Fig. 54. Accuracy and error comparison for piroxicam's C

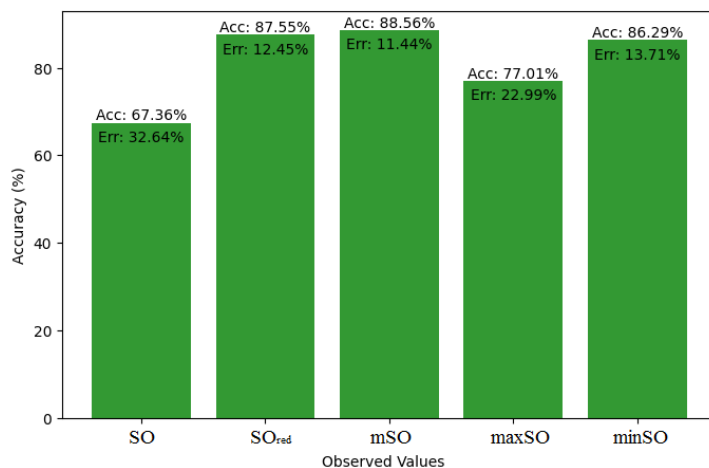


Fig. 55. Accuracy and error comparison for piroxicam's R

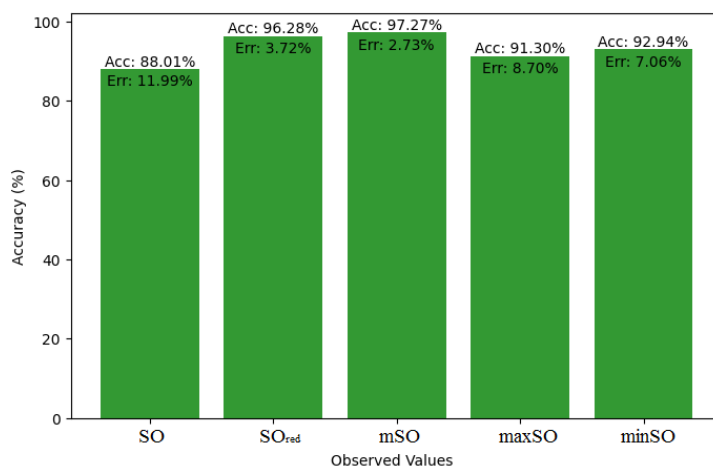


Fig. 56. Accuracy and error comparison for piroxicam's MW

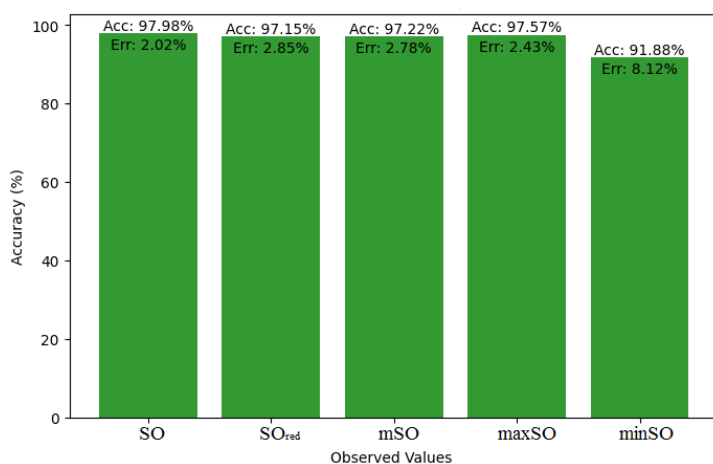


Fig. 57. Accuracy and error comparison for piroxicam's MV

6. Conclusion

The topological index allows for the assignment of a single number to a structure. To understand the connection between property and quantitative structure activity, topological indices need to be

known. Our work shed light on the connections of physicochemical properties of NSAIDs with various Sombor index versions, thereby showing the complex interrelation between these variables. We have ascertained the direction and strength of correlations between specific pharmacological properties and the generated topological indices by using machine learning techniques to compute and analyze the observed values. The following numbers indicate the underlying drugs' best accuracy rate.

Drug	Sombor Verson	Property	Accuracy	Error
Ketorolac	maxSO	C	99.22%	0.78%
Diclofenac	minSO	Pol	99.64%	0.36%
Naproxen	mSO	B.P	99.81%	0.19%
Meloxicam	SO_{red}	R	99.12%	0.88%
Nabumetone	maxSO	MV	99.09%	0.88%
Indomethacin	mSO	R	99.62%	0.38%
Famotidine	minSO	MV	96.03%	3.97%
Etodolac	minSO	R	99.94%	0.05%
Piroxicam	SO_{red}	B.P	99.92%	0.08%

These results are, therefore, very important in our understanding of how physicochemical properties of drugs play a role in the molecular structure and behavior of drugs in biological systems. The results have very practical applications for optimization purposes, medication development, and pharmacological outcome prediction and are, therefore, very important contributions to the pharmaceutical research field. These results can be expanded upon by additional study to improve drug development techniques and the pharmaceutical industry's capacity to provide stronger and more effective medications

Data Availability

Physicochemical properties of drugs have been taken from ChemSpider. research data repositories can be found at www.chemspider.com

Acknowledgements

The authors would like to gratefully acknowledge the critical and constructive comments made by the reviewers which has elevated the standards of the paper significantly. They also acknowledge their co-researcher Ms. Phebe Sarah George for her inputs which refined the content of this paper.

Declarations

The authors declare no conflict of interest.

References

- [1] M. Ajmal, W. Nazeer, M. Munir, S. M. Kang, and C. Y. Jung. The m-polynomials and topological indices of generalized prism network. *International journal of mathematical analysis*, 11(6):293–303, 2017. <https://doi.org/10.12988/ijma.2017.7118>.

- [2] S. Amin, A. U. Rehman Virk, M. Rehman, and N. A. Shah. Analysis of dendrimer generation by sombor indices. *Journal of Chemistry*, 2021(1):9930645, 2021. <https://doi.org/10.1155/2021/9930645>.
- [3] Y. Cao, G. Chen, S. Jiang, H. Liu, and F. Lu. Average degrees of edge-chromatic critical graphs. *Discrete Mathematics*, 342(6):1613–1623, 2019. <https://doi.org/10.1016/j.disc.2019.02.014>.
- [4] X. Chen, M. Li, and F. Lu. Spanning 3-ended trees in quasi-claw-free graphs. *ARS COMBINATORIA*, 138:161–170, 2018.
- [5] L. R. M. Gnanaraj, D. Ganesan, and M. K. Siddiqui. Topological indices and qspr analysis of nsaid drugs. *Polycyclic Aromatic Compounds*, 43(10):9479–9495, 2023. <https://doi.org/10.1080/10406638.2022.2164315>.
- [6] I. Gutman. Topological indices and irregularity measures. *J. Bull*, 8:469–475, 2018. <https://doi.org/10.7251/BIMVI1803469G>.
- [7] I. Gutman. Geometric approach to degree-based topological indices: sombor indices. *MATCH Commun. Math. Comput. Chem*, 86(1):11–16, 2021.
- [8] I. Gutman and K. C. Das. The first zagreb index 30 years after. *MATCH Commun. Math. Comput. Chem*, 50(1):83–92, 2004.
- [9] R. Huang, A. Mahboob, M. W. Rasheed, S. M. Alam, and M. K. Siddiqui. On molecular modeling and qspr analysis of lyme disease medicines via topological indices. *The European Physical Journal Plus*, 138(3):243, 2023. <https://doi.org/10.1140/epjp/s13360-023-03867-9>.
- [10] C.-G. Huo, F. Azhar, A. U. R. Virk, and T. Ismaeel. Investigation of dendrimer structures by means of k-banhatti invariants. *Journal of Mathematics*, 2022(1):4451899, 2022. <https://doi.org/10.1155/2022/4451899>.
- [11] M. N. Husin, S. Zafar, and R. Gobithaasan. Investigation of atom-bond connectivity indices of line graphs using subdivision approach. *Mathematical Problems in Engineering*, 2022(1):6219155, 2022. <https://doi.org/10.1155/2022/6219155>.
- [12] V. Kulli and I. Gutman. Computation of sombor indices of certain networks. *SSRG Int. J. Appl. Chem*, 8(1):1–5, 2021. <https://doi.org/10.14445/23939133/IJAC-V8I1P101>.
- [13] X. Li and Y. Shi. A survey on the randic index. *MATCH Commun. Math. Comput. Chem*, 59(1):127–156, 2008.
- [14] J. Méndez-Bermúdez, R. Aguilar-Sánchez, E. D. Molina, and J. M. Rodríguez. Mean sombor index. *arXiv preprint arXiv:2110.02721*, 2021.
- [15] M. Randić. Quantitative structure-property relationship. boiling points of planar benzenoids. *New journal of chemistry*, 20(10):1001–1009, 1996.
- [16] M. Randić. Characterization of molecular branching. *Journal of the American Chemical Society*, 97(23):6609–6615, 1975. <https://doi.org/10.1021/ja00856a001>.
- [17] M. Randić. Characterization of molecular branching. *Journal of the American Chemical Society*, 97(23):6609–6615, 1975. <https://doi.org/10.1021/ja00856a001>.
- [18] M. Randić. Comparative regression analysis. regressions based on a single descriptor. *Croatica Chemica Acta*, 66(2):289–312, 1993.
- [19] M. Rehman, W. Nazeer, et al. New definition of atomic bond connectivity index to overcome deficiency of structure sensitivity and abruptness in existing definition. *Scientific Inquiry and Review*, 3(4):01–20, 2019. <https://doi.org/10.32350/sir.34.01>.

-
- [20] T. Réti, R. Sharafdini, A. Dregelyi-Kiss, and H. Haghbin. Graph irregularity indices used as molecular descriptors in qspr studies. *MATCH Commun. Math. Comput. Chem*, 79(2):509–524, 2018.
- [21] Z. Shao, M. S. Javed, M. R. Farahani, et al. Degree based graph invariants for the molecular graph of bismuth tri-iodide. *Engineering and Applied Science Letters*, 2(1):1–11, 2019. doi.org/10.30538/psrp-eas12019.0011.
- [22] H. Wiener. Structural determination of paraffin boiling points. *Journal of the American chemical society*, 69(1):17–20, 1947. <https://doi.org/10.1021/ja01193a005>.
- [23] H. Wiener. Structural determination of paraffin boiling points. *Journal of the American chemical society*, 69(1):17–20, 1947. <https://doi.org/10.1021/ja01193a005>.
- [24] W. Yao and L. Li. A new regression model: modal linear regression. *Scandinavian Journal of Statistics*, 41(3):656–671, 2014. <https://doi.org/10.1111/sjos.12054>.
- [25] P. Zhao, F. Lu, V. Voloshin, and K. Diao. On the structure of uniform one-realizations of a given set. *Graphs and Combinatorics*, 34:129–138, 2018. <https://doi.org/10.1007/s00373-017-1866-4>.